

Information transfer and behavioural inertia in starling flocks

Alessandro Attanasi^{1,2}, Andrea Cavagna^{1,2,3*}, Lorenzo Del Castello^{1,2}, Irene Giardina^{1,2,3}, Tomas S. Grigera⁴, Asja Jelić^{1,2*}, Stefania Melillo^{1,2}, Leonardo Parisi^{1,5}, Oliver Pohl^{1,2}, Edward Shen^{1,2}, Massimiliano Viale^{1,2}

¹ *Istituto Sistemi Complessi, Consiglio Nazionale delle Ricerche, UOS Sapienza, 00185 Rome, Italy*

² *Dipartimento di Fisica, Università Sapienza, 00185 Rome, Italy*

³ *Initiative for the Theoretical Sciences, The Graduate Center, City University of New York, 10016 New York, USA*

⁴ *Instituto de Investigaciones Fisicoquímicas Teóricas y Aplicadas (INIFTA) and Departamento de Física, Facultad de Ciencias Exactas, Universidad Nacional de La Plata, c.c. 16, suc. 4, 1900 La Plata, Argentina*
CONICET La Plata, Consejo Nacional de Investigaciones Científicas y Técnicas, Argentina

⁵ *Dipartimento di Informatica, Università Sapienza, 00198 Rome, Italy and*

* *e-mail: asja.jelic@gmail.com, andrea.cavagna@roma1.infn.it*

Appendix A: Border effects

The propagation curve, $x(t)$, namely the distance traveled by the information in a given time, has a linear form only for early and intermediate times, whereas for longer times there is a clear saturation of $x(t)$, Fig. 2. The cause of this saturation is the border of the flocks. To get the propagation curve we have assumed that the number of birds reached by the information, when this has traveled a distance $x(t)$, is proportional to the volume of the sphere with radius x . But this number of birds is exactly the rank $r(t)$ of the last bird reached by the information in a time t , and therefore we have $r(t) \sim x(t)^3$. This argument is true in three dimensions and in the bulk, where no border effects are present.

However, when the information to turn reaches the border of the flock in some direction, things change, as the typical number of birds reached by the information scales with an exponent smaller than 3. To understand this point, let us make the example of flock with a disc-like shape. Once the information has reached the boundary, by traveling a distance equal to the shortest axis, the problem becomes effectively two-dimensional, so that $r(t) \sim x(t)^2$. Similarly, in a tube-shaped flock, one would get $r(t) \sim x(t)$ for long enough times. Hence, in non-spherical systems (as real starling flocks are [1]), we expect in general that for later times, i.e. once the information to turn has reached the boundary, the rank grows like, $r(t) \sim x_{\text{late}}(t)^\alpha$, with $\alpha < 3$. Given that we use a bulk definition of the traveled distance, $x(t) \equiv r(t)^{1/3} \sim x_{\text{late}}(t)^{\alpha/3}$, we expect a saturation of $x(t)$ for later times, due to the fact that $\alpha/3 < 1$. This is indeed what we observe, Fig. 2 and SI-Fig. S3.

Appendix B: The spin

Some theories of collective motion have highlighted the similarity between flocks and magnets [2, 3]. In particular, the Hamiltonian in (2) is the same as that of a

ferromagnet, where the birds velocities \mathbf{v}_i play the role of magnetic spins [3]. However, in previous descriptions spins were only virtual, as they did not obey proper Poisson rules. Within the present description, things change.

The momentum s_z conjugated to the phase φ is defined as the local generator of the rotations parametrized by φ , around the z axis. Hence, (s_z, φ) are generalized action-angle canonical variables. The fact that s_z generates the symmetry parametrized by the phase φ is expressed by Poisson relation, $\{\mathbf{v}, s_z\} = \partial\mathbf{v}/\partial\varphi = i\mathbf{v}$, which in components reads, $\{v_x, s_z\} = \partial v_x/\partial\varphi = -v_y$ and $\{v_y, s_z\} = \partial v_y/\partial\varphi = v_x$. If we interpret v_x and v_y as the x, y components of the spin, these equations show that s_z is a *true* spin, namely the generator of the rotation in the space of the order parameter \mathbf{v} . This is the most general and fundamental definition of spin [4]. Accordingly, $\mathbf{j}_s = \rho_s \nabla\varphi$ is the spin current and $\rho_s = a^2 J$ is the spin stiffness [5].

It is essential to understand that according to this definition s_z is the intrinsic spin, *not* the orbital angular momentum of the bird. Let us define *external* space the space of the birds coordinates and *internal* space (or target space) the space of the order parameter, namely the planar velocity. Indeed, $\mathbf{v}(x, t)$ is a map between the external space $\mathbb{R}^3 \times \mathbb{R}$ and the internal space $\text{SO}(2)$ (the circle). The phase φ parametrizes rotations in the internal space of the velocity and it must not be confused with the orbital angle θ of $2d$ polar coordinates, which parametrizes rotations in the external space of positions. The easiest way to understand this is the following: a bird flying straight (with respect to an arbitrary fixed reference frame - that of our cameras, for example) has $\dot{\varphi} = 0$, but $\dot{\theta} \neq 0$.

As emphasized in the main text, rotations parametrized by these two angles, φ and θ , correspond to two very different types of collective turns. A rotation parametrized by φ corresponds to an *equal radius* turn, i.e. a turn in which all birds have the same radius of curvature and where trajectories cross. On the other hand, a rotation parametrized by θ corresponds to

a *parallel path* turn, typical of rigid bodies. In this kind of turn, paths do not cross and this implies different radii of curvature for different points. The generator of the external θ -rotations is the standard angular momentum, l_z , whereas the generator of the internal φ -rotations is the spin, s_z , which is conserved by the continuity equation.

In order to have some intuition about the physical nature of s_z we must connect external to internal spaces. This connection is established by the kinematic equation,

$$\dot{\mathbf{x}} = v_0 e^{i\varphi}, \tag{B1}$$

expressing the simple fact that birds are not anchored to a lattice, but they follow their velocity vectors. If we consider the speed v approximately constant, equation (B1) implies,

$$\dot{\varphi} = v_0/R, \tag{B2}$$

where R is the instantaneous radius of curvature. Using (6), we also get,

$$\dot{\varphi} = \frac{s_z}{\chi}, \tag{B3}$$

so that we finally have,

$$s_z = \frac{v_0 \chi}{R} \sim \kappa, \tag{B4}$$

where $\kappa = 1/R$ is, by definition, the *curvature* of the trajectory. Therefore, once the connection with the external space is performed, the spin turns out to be essentially the curvature. This is why a bird flying straight ($R = \infty, \kappa \sim 0$) has $s_z \sim 0$, while it has nonzero standard angular momentum l_z . A change (in time) of the spin s_z^i of bird i , due to the social force exerted by the neighbours of i , corresponds to a change (in time) of its instantaneous radius of curvature, R_i , and curvature, κ_i . Hence, what actually propagates across the flock during the turn is a fluctuation (in space and time) of the curvature field, $\kappa(x, t)$. Before the turn, the flock is flying almost straight, $R \gg 1, \kappa \sim 0, s_z \sim 0$. Then the turns sparks in some part of the flock, causing an increase of the curvature κ , i.e. an increase of s_z . This change sweeps through space and time until the whole flock has turned. Finally, after the turn, the flock relaxes back to $R \gg 1, \kappa \sim 0, s_z \sim 0$. Mathematically, this propagation of the curvature, i.e. of s_z , derives from the canonical equations(6): by taking the second derivative with respect to time one obtains a D'Alembert wave equation for $s_z(x, t)$ identical to that obeyed by $\varphi(x, t)$, eq.(8).

Conservation law (7) states that the spin-curvature, $s_z(x, t) \sim \kappa(x, t)$, obeys a continuity equation. As we have seen, this conservation law is crucial to determine sound-like propagation. Continuity means that the trajectory curvature in a given volume cell of the system cannot change unless it is transported into, or out of, that cell by a spin current, $\mathbf{j}_z = \rho_s \nabla \varphi$. We can reformulate this by saying that, if a certain excess of curvature, namely a strong misalignment among a certain

group of individuals, forms in a given point of the system, it cannot be simply dissipated out. Rather, such excitation creates a social force that makes the neighbours turn, and their neighbours too, and so on, so that the excess curvature is transported away, instead of being dissipated.

Finally, note that the spin s_z is *not* the z component of the velocity. Also note that the rotation generated by s_z is the very transformation under which Hamiltonian (5) is symmetric.

Appendix C: The generalized moment of inertia

As we have seen, the spin s_z is not the standard angular momentum l_z . Accordingly, the generalized moment of inertia χ , is not the standard moment of inertia, which in the case of circular motion is, $I = mR^2$, where m is the mass. So, what is the physical and biological meaning of χ ? From the canonical point, the answer is clear: χ is the inertia to changing $\dot{\varphi}$. Indeed, equation (8) can be rewritten as,

$$\chi = \frac{aF_s}{\ddot{\varphi}}, \tag{C1}$$

where $F_s = aJ\nabla^2\varphi$ is the social force exerted by the neighbours. Hence, the generalized moment of inertia χ is *defined* as the ratio between the social force (the cause) and the change of angular velocity (the effect). This is the standard definition of inertia: the ratio between force (cause) and acceleration (effect). However, in this case F_s is a generalized (social) force, and aF_s is a generalized torque, hence χ is not the standard moment of inertia.

To better grasp the biological meaning of χ we must, once again, bridge the gap between internal and external space. By using equations (B1), (B2) and (C1) we obtain several cause-effect relations clarifying the physical and biological meaning of χ . The first relation connects the social force to the change of radius R , or equivalently to the change of curvature κ ,

$$\chi = - \left(\frac{R^2}{v} \right) \frac{aF_s}{\dot{R}} = \left(\frac{1}{v} \right) \frac{aF_s}{\dot{\kappa}}. \tag{C2}$$

Hence, χ is the resistance of a bird to change its instantaneous radius of curvature R (the effect), when a given social force F_s (the cause) is exerted.

Another interesting relation can be obtained in terms of the banking angle γ . A banked turn [6, 7] is the typical way birds (and planes) change their heading. It consists in a gentle roll, so to form an angle γ between the axis of the wings and the horizontal plane. In this way, part of the total lift goes into a centripetal force, $F_c = mg\gamma$, making the bird turn (m is the mass, g the gravitational acceleration and $\gamma \ll 1$). From (C2), it is straightforward to prove that,

$$\chi = \left(\frac{v}{g} \right) \frac{aF_s}{\dot{\gamma}}. \tag{C3}$$

According to (C3), the generalized moment of inertia χ is the resistance of a bird to change its banking angle γ . Here, $\dot{\gamma}$ is the effect of the social force, F_s , and χ sets the ratio between cause and effect. Notice that equations (C2) and (C3) are clearly non-canonical definitions of the inertia χ , because at the denominator they both have a first order derivative in time, rather than a second order one, as in the canonical equation (C1).

Let us emphasize once again that χ is *not* the standard, mechanical moment of inertia, $I = mR^2$, but rather a social, or sensorimotor, resistance of the bird to change R or γ . It is not possible to write an *ab initio* expression for χ in terms of primary mechanical quantities, like mass, radius, etc. To understand this fact, let us imagine that at some point the neighbours of bird i all sharpen their banking angle γ , thus creating a strong social force, $F_s = aJ\nabla^2\varphi$, acting on i . What we call a social ‘force’ is in fact a shortcut to describe a very complex sensorimotor process: a nonzero $\nabla^2\varphi$ means that some of the neighbours of i are now about to crash into i . This is most likely perceived by i , which decides to change its own γ and make it equal to that of the neighbours, thus avoiding the crash. However, the degree by which i will react to the imminent crash, or conversely the resistance to this reaction (which is χ), is the result of a *very* complex trade-off. Let us analyze this trade-off by pretending to be i .

On one side, there is the price of the crash. How imminent is it? This will depend on both the nearest neighbour distance and on the mutual velocity. How bad would that be? Perhaps, I can ignore my neighbours, and just change them, without any real crash. How confident I am into my capability to change γ ? If I am very agile, I can wait a bit longer before changing my γ . On the other side, there is the price to changing γ . How much will it cost me energetically? By increasing γ I will increase the drag against air, otherwise I fall down. But to do this I must increase the power, which is costly. Can I manage to do that?

The generalized moment of inertia χ is the very final product of this very complicated neural and sensorimotor process. Clearly, we cannot know a priori its value. But we can define it, and measure it. This is exactly what we have done by measuring the speed of propagation of the turn across the flock. In this sense, the situation is the same as in real magnetic systems: the parameter χ is the magnetic susceptibility to an external field coupled to s_z [5], which cannot be simply expressed as a function of the microscopic parameters of the theory, but it can be experimentally measured.

Appendix D: Relationship between Φ and J .

The relationship between alignment strength, J , and polarization, Φ , is a consequence of the Gaussian nature of the theory in the spin-wave limit, equation (5). The

polarization is the modulus of the magnetization vector,

$$\Phi = \left\| \frac{1}{N} \sum_i \vec{v}_i \right\|, \quad (\text{D1})$$

so that it has values between 0 and 1 (for simplicity we assume here $\|\vec{v}\| = 1$). Using,

$$\vec{v} = e^{i\varphi}, \quad (\text{D2})$$

and expanding the velocity for small values of the phase, we obtain,

$$\Phi = 1 - \frac{1}{2} \sum_i \varphi_i^2 = 1 - \frac{1}{2} \langle \varphi^2 \rangle. \quad (\text{D3})$$

As expected, the polarization is larger the smaller the phase fluctuations. The small- φ (namely large- Φ) expansion is called spin-wave approximation. We want to remark that spin wave approximation has been found to be accurately verified in real flocks of starlings in previous works [3]. To compute $\langle \varphi^2 \rangle$ we use the fact that in the spin-wave limit the probability distribution of the phase is Gaussian (equation (5)),

$$P(\varphi) \sim \exp\left(-\frac{1}{2}\beta \int \frac{d^3x}{a^3} \rho_s (\vec{\nabla}\varphi)^2\right) \quad (\text{D4})$$

$$= \exp\left(-\frac{1}{2}\beta \int \frac{d^3k}{a^3} \rho_s k^2 \varphi_k \varphi_{-k}\right), \quad (\text{D5})$$

where β is the inverse temperature and the stiffness $\rho_s = a^2J$ is (up to the lattice spacing constant) the strength of the alignment interaction. We therefore have,

$$\Phi(J, \beta) = 1 - \frac{1}{2} \langle \varphi^2 \rangle = 1 - \int d^3k \frac{a}{\beta J k^2} \sim 1 - \frac{1}{\beta J}. \quad (\text{D6})$$

This equation has a rather simple meaning: a large polarization ($\Phi \sim 1$) can be obtained either by reducing the temperature (large β) or by increasing the alignment coupling constant, J . By inverting equation (D6) we get,

$$J = \frac{1/\beta}{1 - \Phi(J, \beta)}. \quad (\text{D7})$$

The fact that J seems to diverge for $\Phi \rightarrow 1$ may be confusing. To understand this point we must keep in mind that Φ is a function of both J and β (eq.(D6)). Hence, the polarization can become very close to 1 even with no divergence of J : this happens if β increases (low temperature) at fixed J , in which case both the numerator and denominator of (D7) go to zero, so that J remains finite. In this case, though, no increase of the second sound speed c_s would be observed, because c_s only depends on J , $c_s^2 = a^2J$. On the other hand, if J increases at constant β , then the polarization Φ approaches 1 and the second sound speed c_s also increases.

Appendix E: Dissipation

According to Noether’s theorem, the spin conservation law is present as long as only even derivatives of the phase with respect to time appear in the equation of motion, as in the D’Alembert equation. Hence, when phase-dissipation occurs, i.e. when a term $\dot{\varphi}$ appears in the equation of motion, strict conservation no longer holds. However, we shall show here that as long as dissipation is low, the qualitative results are the same as in the case of strict conservation. This analysis will also be useful to understand how the diffusive equation of motion (4) derived from the standard theory can be obtained as the overdamped limit of the new theory.

We introduce a dissipative term proportional to $\dot{\varphi}$ in the equation of motion and obtain,

$$\chi \frac{\partial^2 \varphi}{\partial t^2} + \eta \frac{\partial \varphi}{\partial t} - \rho_s \nabla^2 \varphi = 0, \quad (E1)$$

with $\rho_s = a^2 J$ and where η is a generalized friction coefficient. From this we get the dispersion law,

$$\chi \omega^2 - i\eta \omega - \rho_s k^2 = 0. \quad (E2)$$

In the limit $\eta \gg \chi$ we simply get the diffusive result, $\omega = i(\rho_s/\eta)k^2$. In general, however, we obtain,

$$\omega = i \frac{\eta}{2\chi} \pm c_s k \sqrt{1 - k_0^2/k^2}, \quad (E3)$$

where, as usual, the propagation speed is $c_s = \sqrt{\rho_s/\chi}$ and,

$$k_0 \equiv \frac{\eta}{2\sqrt{\rho_s \chi}}. \quad (E4)$$

If we define the dissipation time scale, $\tau \equiv 2\chi/\eta$, and the zero-dissipation frequency, $\omega_0 \equiv c_s k$, we can rewrite the dispersion law as,

$$\omega = i/\tau \pm \omega_0 \sqrt{1 - k_0^2/k^2}. \quad (E5)$$

With zero dissipation, we get $k_0 = 0$, $\tau = \infty$ and $\omega = \omega_0$, which is the case we studied in the main text. For $\eta \neq 0$, on the other hand, we have two regimes, according to the value of the friction coefficient and of the wave number k . For $k \geq k_0$ we have *attenuated* propagating waves, as the frequency has both a real and an imaginary part. For $k < k_0$ we have *overdamped* (or *evanescent*) waves: the frequency is purely imaginary, there is no propagation, but pure exponential decay.

The smallest value of k in the system is $k_{\min} \sim 1/L$, where L is the linear size of the flock. Hence, small dissipation is defined by the relation,

$$\eta < \frac{\sqrt{\rho_s \chi}}{L} : \text{ small dissipation.} \quad (E6)$$

With small dissipation there is linear propagation of the information and the time scale of the exponential decay is set by $\tau = 2\chi/\eta$. From (E6) we get,

$$\tau > \sqrt{\chi/\rho_s} L = L/c_s. \quad (E7)$$

Therefore, small dissipation implies that the damping time constant is larger than the time the information employs to travel across the flock. In other words, the signal is effectively very weakly damped across the length scale of interest. We conclude that even when a small dissipation is present, propagation of information is qualitatively the same as that described by the zero dissipation theory.

We finally note that the existence of a threshold momentum k_0 implies that a continuum theory developed to describe only the asymptotically correct long-wavelength hydrodynamics of a flock, i.e. a theory working in the $k \rightarrow 0$ limit, would miss linear propagation of the phase due to spin conservation, even in very weak damping. This is the case of the hydrodynamic theory of Toner-Tu [8], and its later developments [9].

Appendix F: Dimensional analysis

In the novel theory we have an Hamiltonian that is the sum of two parts. Hence, we have to be careful with physical dimensions. The phase is of course a pure number, $[\varphi] = [1]$, whereas the alignment coupling constant has the dimensions of an energy, $[J] = [e]$. In this way the social force has the dimensions of a true force, $[F_s] = [aJ\nabla^2\varphi] = [e \cdot x^{-1}]$ and the spin has the dimensions of an angular momentum, $[s_z] = [e \cdot t]$, i.e. of an action. Accordingly, χ has the dimensions of a true moment of inertia, $[\chi] = [e \cdot t^2]$. Notice that the term appearing in equation (6) is $a^2 J \nabla^2 \varphi = a F_s$, which is dimensionally a torque. Hence, the derivative of an angular momentum is a torque, as it should.

By definition, the polarization is a pure number, $[\Phi] = [1]$. This is why in the relation linking alignment coupling constant to polarization, $J = 1/[\beta(1-\Phi)]$, we need a dimensional constant with the dimensions of an energy, $[1/\beta] = [e]$. As we have said, $1/\beta$ sets the scale of the noise. Finally, with the above physical dimensions, the speed of propagation of information across the flock, c_s , is measured in meters per second, as it should.

Appendix G: General off-plane case

Our initial assumption that the birds’ velocities lie on a plane during the turn, namely that the turn has very small torsion, although experimentally satisfied (see Fig.1b,c), is not at all a necessary condition for our mathematical description. The most general formulation of our result holds even with a truly 3d order parameter \mathbf{v}_i [5].

If we assume that the mean direction of motion of the flock points in the x direction, then there will be full $3d$ fluctuations of the individual velocities \mathbf{v}_i around the overall direction of motion of the flock, generating small components of \mathbf{v}_i along the two orthogonal axes, z and y . Therefore, we must define two phases, φ_z and φ_y and the Hamiltonian can be spin-wave expanded in terms of these two fields. The phase φ_z parametrizes rotations of \mathbf{v}_i around the z axis (as in the planar - zero torsion case), whereas φ_y parametrizes rotations of \mathbf{v}_i around the y axis. In this fully $3d$ case the Hamiltonian is given by [5],

$$H = \int \frac{d^3x}{a^3} \frac{1}{2} \rho_s \left[(\nabla \varphi_z)^2 + (\nabla \varphi_y)^2 \right] + \frac{1}{2\chi} [s_z^2 + s_y^2], \quad (\text{G1})$$

where $\rho_s = a^2 J$ is, as usual, the stiffness. The equations of motion are,

$$\frac{\partial \varphi_\alpha}{\partial t} = \frac{\delta H}{\delta s_\alpha} = \frac{s_\alpha}{\chi}, \quad (\text{G2})$$

$$\frac{\partial s_\alpha}{\partial t} = -\frac{\delta H}{\delta \varphi_\alpha} = a^2 J \nabla^2 \varphi_\alpha = \nabla \cdot \mathbf{j}_\alpha, \quad (\text{G3})$$

with $\alpha = y, z$, giving rise to two D'Alembert equations,

$$\frac{\partial^2 \varphi_\alpha}{\partial t^2} - c_s^2 \nabla^2 \varphi_\alpha = 0 \quad , \quad c_s^2 = \rho_s / \chi. \quad (\text{G4})$$

In the full $3d$ case we therefore obtain *two*, rather than one, propagating dissipationless modes, along the transverse directions y and z . This is just a manifestation of Goldstone's theorem [10].

These equations are exactly the same as for model G in the Halperin-Hohenberg classification of dynamical universality classes [5, 11]. Model G does not describe superfluid liquid helium, but an isotropic Heisenberg antiferromagnet with staggered magnetization as a non-conserved order parameter, and total magnetization as a constant of motion. An experimental realization of a $3d$ isotropic antiferromagnet is RbMnF_3 , a compound whose dynamics is characterized by the transverse spin-wave modes (G4). Notice that also in this system there is superfluid transport. As discussed in the main text, superfluidity is not restricted to liquid helium II, but it is rather built into the mathematical details of the theory. In particular, it is the product of symmetry and conservation laws. In the full $3d$ case described here (model G) these ingredients give rise to superfluid transport exactly as in the planar (He-II) case.

To write (G1) and (G4) we have assumed that the two excitations φ_z and φ_y are equally likely, so that the only symmetry breaking direction is that of motion. In fact, recent studies on individual diffusion in starling flocks show that gravity is another symmetry breaking direction, heavily suppressing fluctuations along the vertical plane [12]. If we identify z with the axis of gravity, this suppression would imply that rotations of the velocity around the y axis are suppressed, and therefore that φ_y

is less relevant a degree of freedom than φ_z . This suppression induced by gravity is likely the cause of the planar-like turns we observe in flocks and it thus justifies the adoption of the simpler planar description of the main text.

Appendix H: Mutual delay vs reaction time

One may think that the mutual delay between two birds, τ_{ij} , is the same as the reaction time, τ_R , namely the time between the stimulus provided by j and the consequential action of i . However, this is not the case.

Let us assume j is the first bird to turn, and that i is second. By definition of reaction time, i begins its turn τ_R seconds after j . However, we do not define τ_{ij} as the difference between the starting instants of the two turns: there is no practical and robust way to do that, because each birds turns smoothly, so that it is impossible to define the 'start' of the turn. To compute τ_{ij} we use the *entire* trajectory of both birds, by finding the time shift that maximally overlaps the accelerations of i and j (see Fig.1). If the function $a_i(t)$ were *exactly* the same as the function $a_j(t - \tau_{ij})$, then we would have $\tau_{ij} = \tau_R$. This, however, is never the case. First of all there is noise, so that the two curves, $a_i(t)$ and $a_j(t)$, are only approximately shifted with respect to each other. But more importantly, the second bird, i , can try to 'catch up' during the turn, so that the delay at the end of the turn is *shorter* than the delay at the beginning of the turn, which is the reaction time. In this case, the delay τ_{ij} would be a value intermediate between those two times, hence giving a value smaller than τ_R . The opposite can happen too: bird i could in fact lose ground during the turn, so that the delay at the end of the turn is *longer* than the reaction time, and τ_{ij} is larger than τ_R .

EVENT LABEL	N	Φ	c_s (ms ⁻¹)	Δc_s (ms ⁻¹)
20110208.ACQ3	176	0.806	20.20	0.25
20111124.ACQ1	125	0.959	42.64	0.97
20111125.ACQ1	50	0.866	32.38	1.68
20111215.ACQ1	384	0.801	22.74	0.71
20111125.ACQ2	502	0.841	23.86	2.45
20110217.ACQ2	404	0.854	37.70	1.63
20111214.ACQ4.F1	154	0.940	38.46	1.47
20111214.ACQ4.F2.T1	139	0.890	37.32	3.42
20111214.ACQ4.F2.T2	139	0.808	35.40	0.48
20111220.ACQ2	197	0.907	27.54	1.01
20111201.ACQ3.F1	133	0.793	18.82	1.55
20110211.ACQ1	595	0.757	21.96	2.71

TABLE S1. **Polarization and speed of propagation.** N is the number of birds in the flock. The polarization is defined as, $\Phi = \left| \left(\frac{1}{N} \sum_i \mathbf{v}_i / v_i \right) \right|$. The values of Φ reported here are on average smaller than those reported in previous investigations [1, 13]. The reason for this is that previous data were obtained with cameras sampling at 10Hz, whereas the present data are obtained at 170Hz. At this sampling frequency experimental noise and wing flapping reduce the polarization. This reduction, however, affects equally all flocks by uniformly rescaling $(1 - \Phi)$, hence it does not change the correlation in Fig.3. The speed of propagation of the information, c_s , is found by fitting the linear regime of the propagation curve, $x(t)$. The error Δc_s on the speed of propagation c_s is obtained from its variability under changing the linear fitting time interval of $x(t)$.

-
- [1] Ballerini, M., Cabibbo, N., Candelier, R., Cavagna, A., Cisbani, E., Giardina, I., Orlandi, A., Parisi, G., Procaccini, A., Viale, M., & Zdravkovic, V. Empirical investigation of starling flocks: A benchmark study in collective animal behaviour. *Anim. Behav.* **76**, 201–215 (2008).
 - [2] Vicsek, T., Czirók, A., Ben-Jacob, E., Cohen, I., and Shochet, O. Novel type of phase transition in a system of self-driven particles. *Phys. Rev. Lett.* **75**, 1226–1229 (1995).
 - [3] Bialek, W., Cavagna, A., Giardina, I., Mora, T., Silvestri, E., Viale, M. & Walczak, A. M. Statistical mechanics for natural flocks of birds. *Proc. Natl. Acad. Sci. USA* **109**, 4786–4791 (2012).
 - [4] Pauling, L. & Wilson, E. B. *Introduction to quantum mechanics: with applications to chemistry* (McGraw-Hill, New York and London, 1935).
 - [5] Halperin, B.I. & Hohenberg, P.C. Hydrodynamic Theory of Spin Waves. *Phys. Rev.* **188**, 898–918 (1969).
 - [6] Norberg, U. M. *Vertebrate Flight: mechanics, physiology, morphology, ecology and evolution* (Springer Verlag, New York, 1990).
 - [7] Videler, J. J., Birkhead, T. ed. *Avian flight* (Oxford University Press, Oxford, 2005).
 - [8] Toner, J. & Tu, Y. Flocks, herds, and schools: A quantitative theory of flocking. *Phys. Rev. E* **58**, 4828–4858 (1998).
 - [9] Simha, R. A. & Ramaswamy S. Hydrodynamics Fluctuations and Instabilities in Ordered Suspensions of Self-Propelled Particles. *Phys. Rev. Lett.* **89**, 058101 (2002).
 - [10] Goldstone, J. Field Theories with Superconductor Solutions. *Nuovo Cimento* **19**, 154–164 (1961).
 - [11] Hohenberg, P.C. & Halperin, B. I. Theory of dynamic critical phenomena. *Rev. Mod. Phys.* **49**, 435–479 (1977).
 - [12] Cavagna, A., Queirós Duarte, S. M., Giardina, I., Stefanini, F. & Viale, M. Diffusion of individual birds in starling flocks. *Proc. R. Soc. B* **280**, 20122484 (2013).
 - [13] Ballerini, M., Cabibbo, N., Candelier, R., Cavagna, A., Cisbani, E., Giardina, I., Lecomte, V., Orlandi, A., Parisi, G., Procaccini, A., et al. Interaction ruling animal collective behavior depends on topological rather than metric distance: Evidence from a field study *Proc. Natl. Acad. Sci. USA* **105**, 1232–1237 (2008).

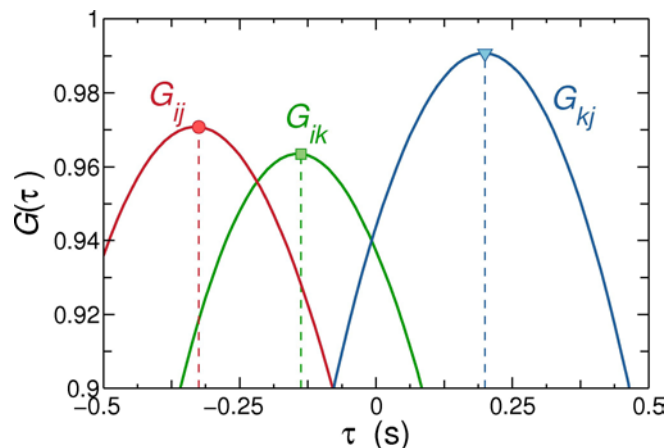


FIG. S1. **Acceleration correlation function.** The correlation function $G_{ij}(\tau)$ measures the overlap between the acceleration of bird i , $a_i(t)$ and the time-shifted acceleration of bird j , $a_j(t - \tau)$, as a function of τ (see Methods). The point where this overlap is maximum corresponds to the delay τ_{ij} between the two birds. In the figure we report the correlation function for a triplet of birds within one of the studied flock.

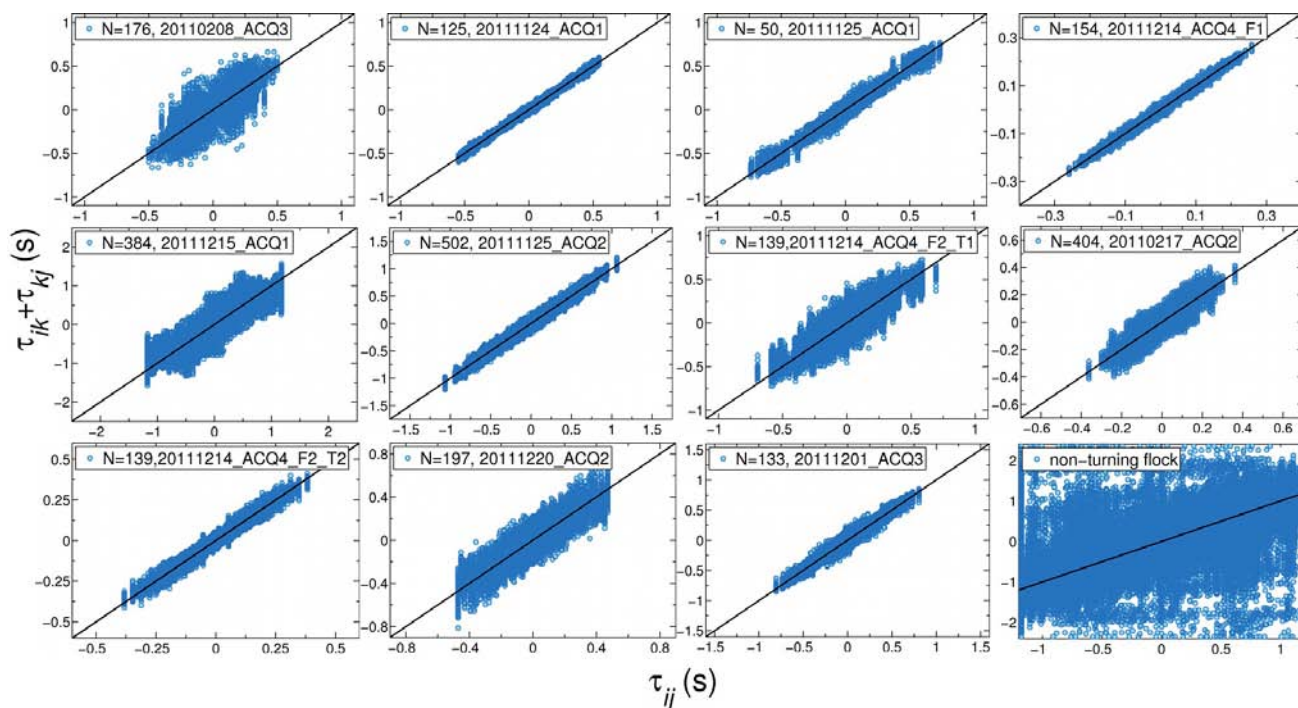


FIG. S2. **Check of the time ordering relation.** We report the time ordering relation test for several of our flocks and for one non-turning flock (lowest-right panel). Temporal consistency requires that $\tau_{ij} \sim \tau_{ik} + \tau_{kj}$, so to have the data scattered along the identity line with clear correlation. In the case of the non-turning flock, on the other hand, the delays are just random numbers, so no temporal consistency is found.

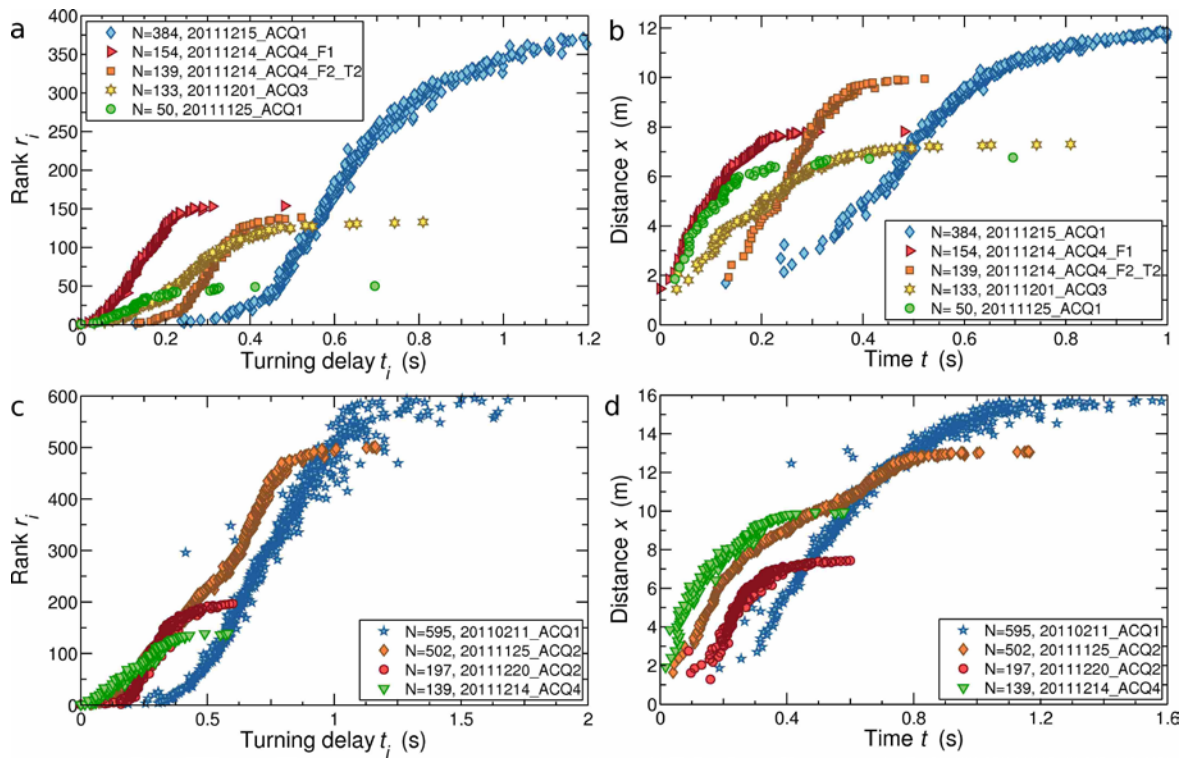


FIG. S3. **Ranking and propagation.** The ranking curve, $r(t)$ (panels (a) and (c)) and the propagation curve, $x(t) = [r(t)/\rho]^{1/3}$ (panels (b) and (d)) are reported for several turning flocks in our pool of data. Together with the data for 3 turning flocks reported in Fig. 2, these represent all the 12 turning events we analyze. The speed of propagation, c_s , is obtained as the slope of the linear regime of $x(t)$ for early and intermediate times (panels (b) and (d)). Moreover, by fitting the ranking curve (panels (a) and (c)) to a power law, $r(t) = t^\alpha$, for early and intermediate times, we find on average $\alpha = 3.2$. Therefore, $x \sim r^{1/3} \sim t^{1.07}$, thus supporting the statement that propagation is linear.